2018 European Control Conference (ECC)
June 12-15, 2018. Limassol, Cyprus

Dissipated energy minimization for an electro-mechanical elevator of a DC microgrid

T.H. Pham, I. Prodan, D. Genon-Catalot, L. Lefèvre

***Abstract*— This paper extends some previous works on the dissipated energy minimization for an elevator system of a DC microgrid using a combination between differential flatness for the reference generation and predictive control for the reference tracking. The contribution of the present work resides in the validation of constraints at all times thanks to the effective use of B-splines parameterization properties. The proposed improvements are validated through simulation and comparison results for a particular electro-mechanical elevator system.**

I. Introduction

Microgrid systems and energy management in general, represent an actual area of research [1]. Many works are providing different modelling and control approaches depending on the global objectives of the corresponding systems. Some works propose predictive control frameworks which take into consideration cost values, power consumption and generation profiles, as well as specific constraints [1]. However, only simplified linear dynamical models for the microgrid components are employed. The energy management task within the microgrid system is generally formulated as a constrained continuous-time optimization problem which is usually difficult to solve.

There are several methods for approximating a continuous-time optimization by a finite-dimensional optimization. An approach for easy implementations is by using the first-order B-splines to parametrize the variables [2]. A drawback of this approach is represented by the fact that the approximated variables do not respect the system dynamics. Thus, higher dimensions are necessary for good approximations, but this requires significant computations. To reduce the computational complexity, the optimization problem can be decomposed into an off-line reference profile generation and an on-line tracking control problem. This is the approach we follow in this work for the optimal control of the electro-mechanical elevator of the DC microgrid illustrated in Fig.1.

In this particular work we focus only on the dissipative energy minimization for the elevator system. In [1] we provide a detail description of the control model of the DC microgrid given in Fig. 1 and solve the load balancing problem. As illustrated in Fig. 1 the electro-mechanical elevator includes the Permanent Magnet Synchronous Machine (PMSM), a mechanical elevator and an AC/DC converter. Usually, the reference profiles of the elevator speed and the motor currents are separately generated. The elevator

T.H. Pham, I. Prodan, D. Genon-Catalot, L. Lefèvre are with Univ. Grenoble Alpes, Grenoble INP*, LCIS, F-26000 Valence, France
thanh-hung.pham@lcis.grenoble-inp.fr
* Institute of Engineering Univ. Grenoble Alpes

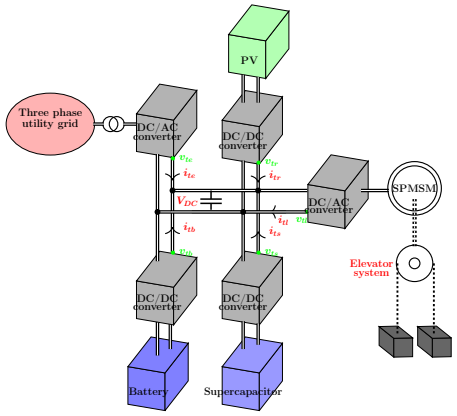

Fig. 1: DC microgrid elevator system.

speed (also the rotor speed) is chosen as a symmetrical trapezoidal curve [3]. In the feasible domain determined by the current and voltage bounds, the motor current references are optimized by minimizing the MTPA (Maximum Torque Per Ampere) criterion [4]. However, this result is useful only for machine speed control, i.e., the effect of the speed profile is not considered for the energy optimization. In [5], the profiles of both stator current and rotor speed are generated in the transient period based on differential flatness [6] with a polynomial parametrization. Note that, no constraints are taken into account. Furthermore, for the PMSM tracking control, various methods are proposed in the literature. A conventional method is the Proportional Integral (PI) control combined with anti-windup techniques for dealing with the physical limits [7]. Another approach is the backstepping method proposed in [8] where the current constraints are tackled by switching the reference speed. In [9] the Interconnection and Damping Assignment Passivity-Based Control (IDA-PBC), an energy-based control method used mainly for nonlinear Port-Controlled Hamiltonian (PCH) systems, was applied for the control of PMSM. However, this approach does not explicitly take into account the constraints. In [10], the authors increase the state vector dimension to obtain a linear system which is used for formulating the tracking Model Predictive Control (MPC). Note that the previously mentioned works do not consider the tracking control for the rotor angle. This is considered in [3] and [5] through the forced dynamics control and adaptive control, respectively, but without taking into account the state and input constraints.

In [11] a constrained predictive control combined with

differential flatness is employed for efficiently managing the dissipative energy. First, optimal profiles of both the stator currents and rotor speed are provided using flat output generation. Next, an MPC-based optimization problem is formulated for tracking the a priori given profiles. However, in [11] the system's constraints are only validated at discrete time instants. Moreover, the elevator position tracking is not considered. Possible ways to overcome these drawbacks are summarized in the following:

- we provide sufficient conditions for the control points describing the B-splines which guarantee the satisfaction of the constraints at all times;
- we consider the rotor angle tracking in the MPC formulation by penalizing its discrepancies in the tracking cost;
- we provide simulation and comparison results which validate the proposed improvements.

II. Problem formulation

This section briefly recalls the optimization-based control formulation for the elevator system in [11]. Next, the reference profile generation is discussed.

A. Optimal control problem formulation

This work aims at minimizing the dissipated energy of the elevator system during an elevator travel while respecting the system dynamics and constraints.

Elevator model: As described in [11], the elevator system is represented by the combination of the AC/DC converter, the PMSM and the mechanical elevator with the following specifications: linear regime of machine, symmetry in the machine construction, non-friction in mechanical system and constant length of the elevator rope. To explicitly describe the power-preserving interconnection and the energy conservation of the elevator system, we express its dynamics using the PCH formalism as[1]:

$$\begin{cases} \dot{\mathbf{x}}(t) &= [\mathbf{J}(\mathbf{x}) - \mathbf{R}(\mathbf{x})]\,\nabla H(\mathbf{x}) + \mathbf{G}(\mathbf{x})\mathbf{u}(t), \\ \mathbf{y}(t) &= \mathbf{G}^T(\mathbf{x})\nabla H(\mathbf{x}), \end{cases} \tag{1}$$

where the state vector, $\mathbf{x}(t) = [x_1(t) \quad x_2(t) \quad x_3(t)]^T \in \mathbb{R}^3$, represents the direct and quadrature stator fluxes and the mechanical momentum. The input vector, $\mathbf{u}(t) = [u_1(t) \quad u_2(t) \quad u_3(t)]^T \in \mathbb{R}^3$, describes the direct and quadrature stator voltages and the mechanical torque caused by the gravity. The output vector, $\mathbf{y}(t) = [y_1(t) \quad y_2(t) \quad y_3(t)]^T \in \mathbb{R}^3$, denotes the direct and quadrature stator currents and the motor speed. The interconnection matrix, $\mathbf{J}(\mathbf{x}) \in \mathbb{R}^{3\times3}$, the resistive matrix, $\mathbf{R}(\mathbf{x}) \in \mathbb{R}^{3\times3}$ and the input matrix, $\mathbf{G}(\mathbf{x}) \in \mathbb{R}^{3\times3}$, are given by:

$$\begin{cases} \mathbf{J}(\mathbf{x}) = \begin{bmatrix} 0 & 0 & x_2(t) \\ 0 & 0 & -x_1(t) \\ -x_2(t) & x_1(t) & 0 \end{bmatrix}, \\ \mathbf{R}(\mathbf{x}) = \text{diag}\,\{R_l, R_l, 0\},\ \mathbf{G}(\mathbf{x}) = \mathbf{I}_3, \end{cases} \tag{2}$$

where R_l is the phase resistance of the machine stator. The Hamiltonian describes the magnetic energy in PMSM stator and the kinematic energy in the mechanical elevator:

$$H(\mathbf{x}) = \mathbf{Q}_0 + \mathbf{Q}_1^T\mathbf{x}(t) + \frac{1}{2}\mathbf{x}^T(t)\mathbf{Q}_2\mathbf{x}(t), \tag{3}$$

with $\mathbf{Q}_0 \in \mathbb{R}$, $\mathbf{Q}_1 \in \mathbb{R}^{3\times1}$ and $\mathbf{Q}_2 \in \mathbb{R}^{3\times3}$.

Constraints: This work considers some typical constraints for the elevator system on the motor currents, $y_1(t)$, $y_2(t)$, the motor speed, $y_3(t)$, the motor voltages, $u_1(t)$, $u_2(t)$, and the mechanical torque, $u_3(t)$, such as:

$$\mathbf{y}(t) \in \mathbb{G}_y,\ \mathbf{u}(t) \in \mathbb{G}_u,\ \forall t \in [t_0, t_f], \tag{4}$$

where $\mathbb{G}_y,\ \mathbb{G}_u \subset \mathbb{R}^3$ are convex sets defined by:

$$\mathbb{G}_y = \left\{ \mathbf{y}(t) \in \mathbb{R}^3 \;\middle|\; \begin{array}{l} y_1^2(t) + y_2^2(t) \le \dfrac{I_{max}^2}{2}, \\ \omega_{min} \le y_3(t) \le \omega_{max} \end{array} \right\}, \tag{5a}$$

$$\mathbb{G}_u = \left\{ \mathbf{u}(t) \in \mathbb{R}^3 \;\middle|\; \begin{array}{l} u_1^2(t) + u_2^2(t) \le \dfrac{v_{ref}^2}{2}, \\ u_3(t) = \Gamma_{res} \end{array} \right\}, \tag{5b}$$

where I_{max} is the maximal current magnitude, ω_{min}, ω_{max} are the minimal and maximal rotor speeds, v_{ref} is the DC bus voltage at one side of the converter, Γ_{res} is the gravity torque[2].

In (4) the initial and final elevator speeds and the rotor angle fulfill the following constraints:

$$y_3(t_0) = y_3(t_f) = 0, \tag{6a}$$

$$\theta(t_f) = \theta_f,\ \text{with}\ \theta(t) = \int_{t_0}^{t} y_3(t)dt, \tag{6b}$$

where θ_f is the required rotor angle during an elevator travel.

Objective: Considering the PCH elevator dynamics (1), we derive the dissipated energy within the system during the elevator travel as:

$$V(\mathbf{x}) = \int_{t_0}^{t_f} \nabla^T H(\mathbf{x})\mathbf{R}(\mathbf{x})\nabla H(\mathbf{x})dt. \tag{7}$$

Hence, we formulate the optimal control problem for the elevator system as:

$$\begin{aligned} \overline{\mathbf{u}}(t) = &\ \underset{\mathbf{u}(t)}{\text{argmin}}\ V(\mathbf{x}), \\ \text{subject to} &\begin{cases} \text{dynamics (1)-(3)}, \\ \text{constraints (4)-(6b)}. \end{cases} \end{aligned} \tag{8}$$

Note that the optimization problem (8) is in continuous-time. In [11], it is approximated by a combination of off-line reference profile generation and on-line reference tracking using differential flatness with B-splines parameterization and MPC.

[1] [12] provides the Port-Hamiltonian-based modelling of the global microgrid system which takes into account all the physical properties of the grid.

[2] Considering the gravity torque as a known parameter leads to complex expressions of the state end input in terms of the flat output. Thus, it may be impractical to provide conditions for the continuous-time constraint validation.

B. *Reference profile generation*

This subsection uses the differential flatness and B-splines parametrization tools for the reference profile generation.

Proposition 1: The dynamical PCH system given in (1)-(3) is differentially flat with the flat output:

$$\mathbf{z}(t) = \mathbf{y}(t) \in \mathbb{R}^3. \tag{9}$$

Proof: In (2)-(3), we notice two following characteristics: i) the input matrix, $\mathbf{G}(\mathbf{x})$, is constant and invertible; ii) the Hamiltonian, $H(\mathbf{x})$, is quadratic and positive. Thus, using the definition of the flatness [6], we can easily verify that the elevator system (1)-(3) is flat with the flat output $\mathbf{z}(t)$ in (9). Using this flat output, the state, $\mathbf{x}(t)$, and control, $\mathbf{u}(t)$, variables can be algebraically expressed in term of $\mathbf{z}(t)$ and its derivative:

$$\mathbf{x}(\mathbf{z}(t)) = \mathbf{Q}_2^{-1}\left(\mathbf{z}(t) - \mathbf{Q}_1\right), \tag{10a}$$

$$\mathbf{u}(\mathbf{z}(t), \dot{\mathbf{z}}(t)) = \mathbf{A}\dot{\mathbf{z}}(t) + \mathbf{B}\mathbf{z}(t) + \sum_{k=1}^{3} z_k(t)\mathbf{C}_k\mathbf{z}(t), \tag{10b}$$

where $\mathbf{A}, \mathbf{B}, \mathbf{C}_k \in \mathbb{R}^{3\times 3}$ are the appropriate constant matrices, $z_k(t) \in \mathbb{R}$ is the k^{th} coordinate of the flat output, $\mathbf{z}(t)$. Moreover, through the presented proof, we verify the fact that a controllable system is flat [6]. ■

Remark 1: Note that, by using the flat output (9), we reduce the number of variables considered in the optimization problem (8) (i.e., 3 flat outputs instead of 3 state variables and 3 input variables). Furthermore, it guarantees that the generated reference profiles respect the system dynamics. ■

Next, we choose to use B-splines to parameterize the flat output, $\mathbf{z}(t)$, due to the ease of computing their derivatives. Moreover, their degree depends only up to which derivative is needed to ensure continuity. Thus, we consider in the following that the flat output is projected over N B-splines of order d:

$$\mathbf{z}(t) = \sum_{j=1}^{N} \mathbf{p}_j \lambda_{j,d}(t) = \mathbf{P}\Lambda_d(t), \tag{11}$$

where $\mathbf{p}_j \in \mathbb{R}^3$ is the j^{th} control point. The control point matrix, $\mathbf{P} \in \mathbb{R}^{3\times N}$, gathers N control points as:

$$\mathbf{P} = \left[\mathbf{p}_1\ \mathbf{p}_2\ \dots\ \mathbf{p}_N\right], \tag{12}$$

$\lambda_{j,d}(t) \in \mathbb{R}$ denotes the j^{th} B-spline of order d defined by a recursive formula over a knot-vector $\mathbb{T} \in \mathbb{R}^{N+d}$ [13], which gathers transient time instants, $\tau_j \in [t_0, t_f]$, as:

$$\mathbb{T} = \{\tau_0 \leq \tau_1, \dots, \tau_{N+d}\}, \tag{13}$$

with $\tau_0 = \tau_1 = \dots = \tau_{d-1} = t_0$, $\tau_{N+1} = \tau_{N+2} = \dots = \tau_{N+d} = t_f$. Furthermore, in (11) $\Lambda_d(t) \in \mathbb{R}^N$ is the B-spline vector gathering N B-splines, i.e., $\Lambda_d(t) = \left[\lambda_{1,d}(t)\ \lambda_{2,d}(t)\ \dots\ \lambda_{N,d}(t)\right]^T$.

Substituting the parameterizations (9)-(11) in the continuous-time optimization problem (8), we obtain a new optimization problem with finite-dimensional arguments, i.e., the control points in (12). However, the obtained constraints explicitly depend on time, this requires a continuous-time validation. Furthermore, the discrete cost derived from (1)-(3), (7) and (9)-(11) is also an explicit function of time. Thus, the derived optimization problem is difficult for numerical implementation.

Remark 2: In [11], the obtained constraints are verified at some chosen instants while the derived discrete cost function is approximated by a discrete sum. Note that this approach is simple to implement but is not complete since it provides no guarantees for the intra-sample behavior. ■

By solving the optimization problem (8), we obtain the reference profiles for the state, input and output variables. The profiles will be tracked using MPC as described in the next subsection.

III. Continuous constraint validation and position tracking

In this section, we propose solutions for overcoming the limitations presented in Remark 2.

A. *Continuous constraint validation*

By taking into account the properties of the B-splines, the continuous-time constraints of the elevator system are validated at all times.

First, using (1)-(3), (7), (9) and (11), we obtain a quadratic cost function:

$$V(\mathbf{P}) = \sum_{i=1}^{N}\sum_{j=1}^{N} \mathbf{p}_i^T \mathbf{R}_{i,j} \mathbf{p}_j, \tag{14}$$

where $\mathbf{R}_{i,j} \in \mathbb{R}^{3\times 3}$ with $i, j = 1, \dots, N$ are the appropriate weight matrices.

Note that, rewriting (5b) using the defined control points in (11), we see that the control points must satisfy an equality constraint with nonlinear terms. This is not easy to implement and leads to a numerically cumbersome formulation. Hereinafter, we rewrite the optimization problem above (8) as a soft constrained optimization problem where we penalize in the cost a slack variable ϵ:

$$\overline{\mathbf{P}} = \underset{\mathbf{P},\epsilon}{\operatorname{argmin}}\ V(\mathbf{P}) + Q_\epsilon \epsilon, \tag{15}$$

$$\text{subject to } \begin{cases} \text{constraints (4), (6a)-(6b), (9)-(11),} \\ \mathbf{u}\left(\mathbf{z}(t), \dot{\mathbf{z}}(t)\right) \in \mathbb{G}_{u\epsilon}, \\ \epsilon \geq 0, \end{cases} \tag{16}$$

where the set $\mathbb{G}_u$ in (5b) is rewritten as:

$$\mathbb{G}_{u\epsilon} = \left\{ \mathbf{u}(t) \in \mathbb{R}^3 \;\middle|\; \begin{array}{l} u_1^2(t) + u_2^2(t) \leq \dfrac{v_{ref}^2}{2}, \\ |u_3(t) - \Gamma_{res}| \leq \epsilon \end{array} \right\}, \tag{17}$$

where $Q_\epsilon \in \mathbb{R}$ ia a positive coefficient and $\epsilon \in \mathbb{R}$ is a relaxation factor.

In the following, sufficient conditions for the control points are formulated to guarantee the satisfaction of the system constraints (4)-(6b) written in function of the flat output (9)-(11).

Proposition 2: Let the following conditions be satisfied:

$$p_{3,1} = p_{3,N} = 0, \tag{18a}$$

$$\sum_{j=1}^{N} p_{3,j} \int_{t_0}^{t_f} \lambda_{j,d}(t)dt = \theta_f, \tag{18b}$$

$$\mathbf{p}_j \in \mathbb{G}_y, \tag{18c}$$

$$\mathbf{p}_{l,i,j} \in \mathbb{G}_{u\epsilon}, \tag{18d}$$

with $d-1 \leq l \leq N+d$ the B-spline time interval index $[\tau_{l-1}, \tau_l]$, $l-d+1 \leq i,j \leq l$. $\mathbf{p}_j \in \mathbf{R}^3$ denote the j^{th} control point, $p_{k,i} \in \mathbf{R}$ denotes the k^{th} coordinate of the i^{th} control point. $\mathbb{G}_y$, $\mathbb{G}_{u\epsilon}$ are the convex sets defined in (5) and (17). The short notation $\tilde{\mathbf{p}}_{l,i,j} \in \mathbb{R}^3$ is defined as:

$$\tilde{\mathbf{p}}_{l,i,j} = \mathbf{APM}_{d,d-1}\mathbf{S}_{l,d-1,d,i} + \mathbf{B}\mathbf{p}_i + \sum_{k=1}^{3} p_{k,i}\mathbf{C}_k\mathbf{p}_j, \tag{19}$$

where $\mathbf{P} \in \mathbf{R}^{3\times N}$ denotes the control point matrix in (11). $\mathbf{A}$, $\mathbf{B}$, $\mathbf{C}_k$ are defined in (10). Also, $\mathbf{M}_{d,d-1} \in \mathbb{R}^{N\times(N-1)}$ describes the relations between the first derivatives of the B-splines of order d and the B-splines of order $d-1$. $\mathbf{S}_{l,d-1,d,i} \in \mathbb{R}^{N-1}$ describes the relations of the B-splines of order $d-1$ and the i^{th} B-spline of order d over the time interval $[\tau_{l-1}, \tau_l]$. Then, the continuous-time constraints (16) are satisfied. □

Proof: (i) Note that $\lambda_{1,d}(t_0) = 1$ and $\lambda_{i,d}(t_0) = 0$ with $i = 2, \ldots, N$. Similarly, $\lambda_{N,d}(t_0) = 1$ and $\lambda_{i,d}(t_f) = 0$ with $i = 1, \ldots, N-1$. Thus, (18a) implies the constraint (6a).
(ii) Since, the parameterization (11) is linear, we can easily derive the condition (18b) for the control points from the angle constraint (6b), the flat output choice (9) and the parameterization (11).
(iii) An important B-spline property is the unity partition condition, i.e., each B-spline is non negative, and the sum of B-splines is the unity. Thus, the spline curve $\mathbf{z}(t)$ remains in the convex hull of the control points. Therefore, if all control points belong to the convex set $\mathbb{G}_y$, $\mathbf{z}(t)$ belong to $\mathbb{G}_y$. Thus, the continuous-time constraint (4) is satisfied.
(iv) Consider the time interval $[\tau_{l-1}, \tau_l]$. Let $\beta_{i,j,d}(t) = \lambda_{i,d}(t)\lambda_{j,d}(t)$ with $1 \leq i,j \leq N$. From the parameterization (11) and B-splines properties given in [13], we obtain:

$$\mathbf{z}(t) = \sum_{i=1}^{N}\sum_{j=1}^{N} \mathbf{p}_i \beta_{i,j,d}(t), \tag{20a}$$

$$\dot{\mathbf{z}}(t) = \sum_{i=1}^{N}\sum_{j=1}^{N} \mathbf{PM}_{d,d-1}\mathbf{S}_{l,d-1,d,i}\beta_{i,j,d}(t). \tag{20b}$$

Substituting the parameterization (11) to the third term of the input, $\mathbf{u}(t)$, in (10), we derive:

$$\sum_{k=1}^{3} z_k(t)\mathbf{C}_k\mathbf{z}(t) = \sum_{i=1}^{N}\sum_{j=1}^{N}\sum_{k=1}^{3} p_{k,i}\mathbf{C}_k\mathbf{p}_j\beta_{i,j,d}(t). \tag{21}$$

Using (20)-(21), we express the input, $\mathbf{u}(t)$, in (10) as:

$$\mathbf{u}(t) = \sum_{i=1}^{N}\sum_{j=1}^{N} \tilde{\mathbf{p}}_{l,i,j}\beta_{i,j,d}(t). \tag{22}$$

Since $\beta_{i,j,d}(t)$ with $l-d+1 \leq i,j \leq l$ satisfies the unity partition condition, $\mathbf{u}(t)$ remains in the convex hull of $\{p_{l,i,j}\}$ with $l-d+1 \leq i,j \leq l$. Thus, if $\{p_{l,i,j}\}$ with $l-d+1 \leq i,j \leq l$ belong to the convex set $\mathbb{G}_{u\epsilon}$ as in (18d), the input $\mathbf{u}(t)$ remains in $\mathbb{G}_{u\epsilon}$. This implies that the second continuous-time constraint in (16) is satisfied. Consequently, the presented proof shows that the constraints (16) are satisfied if the constraints (18) are satisfied. ■

Once we obtain the optimal control points described by $\overline{\mathbf{P}}$ in (15)-(17), we can generate the reference profiles for the system outputs, $\overline{\mathbf{y}}(t)$, representing the motor currents and the elevator speed, thanks to (9) and (11). Also, we derive the input reference profiles, $\overline{\mathbf{u}}(t)$, representing the motor voltages thanks to (10)-(11). Moreover, we determine the reference profile of the rotor angle, $\overline{\theta}(t)$, thanks to (6b), (9) and (11). Next, the generated feasible references which respect the system dynamics and constraints will be tracked using MPC.

B. *Position tracking with linearized system dynamics*

In this subsection, we consider a MPC law for tracking the motor angle reference of the elevator system. To simplify the MPC optimization problem, the elevator dynamics (1) are linearized. Let the discrepancies between the actual state, input, output and rotor angle variables, $\mathbf{x}(t) \in \mathbb{R}^3$, $\mathbf{u}(t) \in \mathbb{R}^3$, $\mathbf{y}(t) \in \mathbb{R}^3$, $\theta(t) \in \mathbb{R}$ and their references, $\overline{\mathbf{x}}(t)$, $\overline{\mathbf{u}}(t)$, $\overline{\mathbf{y}}(t)$, $\overline{\theta}(t)$, be denoted by $\tilde{\mathbf{x}}(t)$, $\tilde{\mathbf{u}}(t)$,$\tilde{\mathbf{y}}(t)$ and $\tilde{\theta}(t)$. Therefore, from (1)-(3), (6b) and $\mathbf{x}(t) \approx \overline{\mathbf{x}_l}(t)$, we obtain the linearized discrepancy dynamics:

$$\begin{cases} \dot{\tilde{\mathbf{x}}}(t) = & [\mathbf{J}(\overline{\mathbf{x}}) - \mathbf{R} - \mathbf{S}(\overline{\mathbf{x}})]\,\mathbf{Q}_2\tilde{\mathbf{x}}(t) + \mathbf{G}\tilde{\mathbf{u}}(t), \\ \tilde{\mathbf{y}}(t) = & \mathbf{G}^T\mathbf{Q}_2\tilde{\mathbf{x}}(t), \\ \tilde{\theta}(t) = & \int_{t_0}^{t} \tilde{y}_3(t)dt. \end{cases} \tag{23}$$

where $\mathbf{S}(\overline{\mathbf{x}}) \in \mathbb{R}^{3\times 3}$ is defined as:

$$\mathbf{S}(\overline{\mathbf{x}}) = \begin{bmatrix} \mathbf{J}_1\nabla H(\overline{\mathbf{x}}) & \mathbf{J}_2\nabla H(\overline{\mathbf{x}}) & \mathbf{J}_3\nabla H(\overline{\mathbf{x}}) \end{bmatrix}, \tag{24}$$

with $\mathbf{J}_1, \mathbf{J}_2, \mathbf{J}_3 \in \mathbb{R}^{3\times 3}$ such that:

$$\mathbf{J}(\mathbf{x}) = \mathbf{J}_1 x_1(t) + \mathbf{J}_2 x_2(t) + \mathbf{J}_3 x_3(t). \tag{25}$$

Note that the linearized dynamics (23) is a time-varying linear system since the reference state variable, $\mathbf{x}(t)$, explicitly depend on time.

We consider the recursive construction of an optimal open-loop control sequence, $\tilde{\mathbf{U}}(t) = \{\tilde{\mathbf{u}}(t|t), \ldots, \tilde{\mathbf{u}}(t+N_p-1|t)\}$, at instant t over a finite prediction horizon, N_p, which leads to a feedback control policy by the effective application of the first control action as the system input:

$$\tilde{\mathbf{U}}^*(t) = \underset{\tilde{\mathbf{U}}(t)}{\operatorname{argmin}}\ V_m(\tilde{\Theta}, \tilde{\mathbf{U}}) \tag{26a}$$

$$\text{subject to } \begin{cases} \text{discretized dynamics of (23),} \\ \text{discretized constraints of (4),} \end{cases} \tag{26b}$$

where $\tilde{\Theta} = \{\tilde{\theta}(t|t), \ldots, \tilde{\theta}(t+N_p-1|t)\}$ is the rotor angle sequence, $V_m(\tilde{\Theta}, \tilde{\mathbf{U}})$ penalizes the discrepancies between the rotor angle, the stator voltages and their references:

$$V_m(\tilde{\Theta}, \tilde{\mathbf{U}}) = \sum_{s=0}^{N_p-1} k_0\tilde{\theta}(t+s|t)^2 + \|\tilde{\mathbf{u}}_l(t+s|t)\|_{\mathbf{Q}_u}, \tag{27}$$

where $k_0 \in \mathbb{R}$ and $\mathbf{Q}_u \in \mathbb{R}^{3\times 3}$ are the weight matrices. Note that due to the equality constraint of the mechanical torque of the elevator gravity, $u_3(t)$, of the input vector, $\mathbf{u}(t)$, in (4), the third coordinate, $\tilde{u}_3(t)$, of the input discrepancy vector, $\tilde{\mathbf{u}}(t)$, is equal to zero. Moreover, the implemented MPC is not linear since the time-varying linear dynamics is updated during the prediction horizon.

Remark 3: For the discretization of the PCH system (1) we presented in [11] a discretization method which preserves the energy conservation and the power-preserving interconnection of the elevator system. We choose not to detail here the proposed discretization approach since this is not the main goal of this paper. ■

IV. Simulation Results

This section presents simulation and comparison results for the reference profile generation and their tracking using the approach proposed above. The model parameters are presented in Table I with the numerical data given by the industrial partner SODIMAS (an elevator company from France). The table also presents the simulation setting. Two simulation scenarios are considered here: (a) perturbation-affected dynamics with feedforward control, (b) perturbation-affected dynamics with MPC. Physically, these perturbations represent strong interactions between the system and the environment during a short time duration (much shorter than the time step). By modifying the state variables, it also modifies the system stored energy, $H(\mathbf{x})$ in (3). For the simplicity, we do not consider here the uncertainty on the control variables, on the feedback (output) signals and on the model parameters. The perturbation are summarized in Table II. The numerical optimization problem is solved by using Yalmip and IPOPT [14] solvers in Matlab 2013a.

TABLE I: System parameters and simulation setting.

Name	Notation	Value
System parameters		
Stator resistance	R_l $[\Omega]$	0.53
Gravity torque	Γ_{res} $[N.m]$	149
Maximal current magnitude	I_{max} $[A]$	41.2
DC-link voltage	v_{ref} $[V]$	400
Maximal angular speed	ω_{max} $[rad/s]$	29.6
Minimal angular speed	ω_{min} $[rad/s]$	0
Initial rotor angle	θ_0 $[rad]$	0
Final rotor angle	θ_f $[rad]$	592.6
Hamiltonian weight matrices	$\mathbf{Q}_0$ $[J]$	8325.1
	$\mathbf{Q}_1$	$[-129.0 \quad 0 \quad 0]^T$
	$\mathbf{Q}_2$	diag {111.6, 89.0, 0.3}
Simulation setting		
Time interval	$[t_0, t_f]$ $[s]$	$[0, 30]$
B-spline number	N	10
B-spline order	d	5
Soft constraint weight	Q_ϵ $[(Nm)^{-1}]$	10^5
Discrete time step	h $[s]$	0.001
Prediction horizon	N_p	1
Input weight matrix	$\mathbf{Q}_u$	$\mathbf{I}_3$

Reference profile generation: Different B-splines orders and numbers are considered and compared using two criteria: computation time and torque error. We see that with 8 B-splines of order 5 the soft constraint technique gives the smallest torque error and the shortest time computation. They are used to generate the reference profiles of the output currents, $\overline{y_1}(t), \overline{y_2}(t)$, the rotor speed, $\overline{y_3}(t)$, and the rotor angle, $\overline{\theta}(t)$, as illustrated in Fig. 2 by the solid lines. They are obtained by solving the constrained optimization problem (15) subject to (16), (18). We show in this figure that the constraints on the currents, on the voltages and on the rotor speed (the dashed lines) are respected at all times.

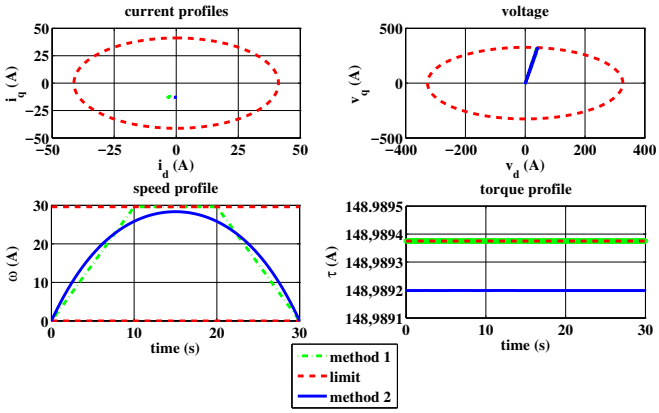

Fig. 2: Reference profiles for the currents, voltages, rotor speed and magnetic torque.

Comparison results: We consider two following reference generation methods. Method 1 uses trapezoidal rotor speed profiles with the MTPA method [3]. Method 2 uses differential flatness with the B-splines parametrization. The reference profiles obtained with our approach (Method 2) respect the elevator dynamics and provide a lower dissipated energy (2647 J), which is not the case for the MTPA method (2709 J).

TABLE II: Perturbations values for the two scenarios.

Case	Current	Speed	Angle
(a)	9 $[A]$	-1.2 $[rad/s]$	1 rad
(b)	0 $[A]$	-1.2 $[rad/s]$	0 rad

Reference tracking: Next, the feasible references obtained above are tracked using MPC. The generated control references are first applied to the perturbation-affected system in case (a) (see also Table II). From the obtained results, we note that the dynamics of the two currents and the speed are asymptotically stable around the corresponding reference profiles. However, the discrepancy between the rotor angle and its reference is constant. This causes the angle errors at the end of the elevator travel.

The previous simulation results for the feedforward control motivate us to concentrate on the rotor angle tracking in the MPC formulation. Note that when the rotor angle discrepancy converges to zero, the rotor speed discrepancy will increase which may overpass the speed limitation. This problem is especially important when the perturbation affects the system at the instant $t = 15$ s when the motor speed and the voltages are closer to the boundary (illustrated in

Fig.2). Based on the simulations for the open-loop system, we consider some simplifications for the tracking control problem such as: i) only the discrepancies of the rotor angle and of the stator voltages are penalized in the MPC cost (see (27)); ii) only the perturbation on the motor speed is considered; iii) one-step MPC is considered, i.e., $N_p = 1$. The controller parameters are enumerated in the Table I.

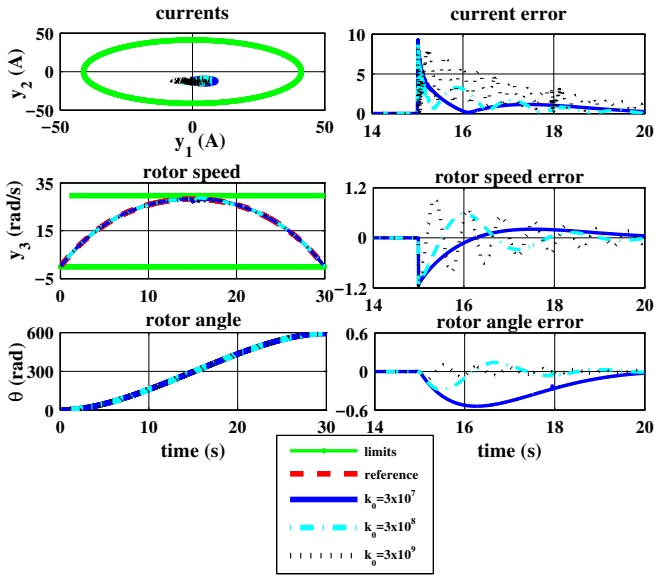

Fig. 3: Time evolutions and errors of the output variables and of the rotor angle in case (b).

Figures 3 describes the time evolution and the discrepancies of the output and the rotor angle for the case of the perturbation-affected dynamics with the MPC formulated in (26a)-(27). We observe that the proposed tuning MPC parameters guarantee the asymptotic stability of the electro-mechanical elevator system at the generated reference profiles. Moreover, increasing the angle weight parameter, k_0, increases the vibration of the state discrepancies but can not reduce the convergence time. This drawback may be overcome by penalizing the speed and current discrepancies in the tracking cost, V_m, in (27). Also, the convergence time in the tracking control problem can be reduced by adding a quadratic function of the current and speed errors to the MPC cost and/or modifying the prediction horizon. Table III shows that the dissipated energy increases when k_0 increases.

TABLE III: Dissipated energy.

Case	(a)	$k_0 = 3.10^7$	$k_0 = 3.10^8$	$k_0 = 3.10^9$
Energy [J]	2647.1	2647.3	2648.5	2669.1

V. Conclusions

This paper presented an optimization-based control design for the dissipated energy minimization of the elevator system while respecting the system dynamics and constraints. An efficient combination among differential flatness, B-spline parameterization and tracking Model Predictive Control was employed and validated through simulations and comparisons. Briefly, the developments of this work are summarized as: i) the elevator constraints are validated at all times thanks to specific properties of the B-splines parametrization; ii) the position reference is tracked using an additional term of the rotor angle discrepancy to the Model Predictive Control cost function. The short term future work is concentrating on the satisfaction of the equality constraint of the mechanical torque in the reference profile generation which will be tackled by using appropriate B-splines parametrization instead of the soft constraint technique.

Acknowledgement

This work has been partially funded by the European Artemis ARROWHEAD project under grant agreement number 332987.

References

[1] T. Pham, I. Prodan, D. Genon-Catalot, and L. Lefèvre, "Power balancing in a DC microgrid elevator system through constrained optimization," in *20th World Congress of the International Federation of Automatic Control*, vol. 50, no. 1. IFAC, July 2017, pp. 19–24.

[2] M. Ellis, J. Liu, and P. Christofides, *Economic Model Predictive Control*. Springer, 2017.

[3] J. Vittek, P. Butko, B. Ftorek, P. Makys, and L. Gorel, "Energy near-optimal control strategies for industrial and traction drives with AC motors," *Mathematical Problems in Engineering*, 2017.

[4] J. Lemmens, P. Vanassche, and J. Driesen, "PMSM drive current and voltage limiting as a constraint optimal control problem," *the IEEE Journal of Emerging and Selected Topics in Power Electronics*, vol. 3, no. 2, pp. 326–338, April 2014.

[5] K.-Y. Chen, M.-S. Huang, and R.-F. Fung, "Adaptive minimum-energy tracking control for the mechatronic elevator system," *IEEE Trans. on Control Systems Technology*, vol. 25, no. 5, pp. 1790 – 1799, 2013.

[6] M. Fliess, J. Lévine, and P. Rouchon, "Flatness and defect of non-linear systems: Introductory theory and examples," *International journal of control*, vol. 61, pp. 1327–1361, 1995.

[7] M. Mardaneh, F. Bavafa, S. Alavi, and M. Sadeghi, "Nonlinear PI controller for interior permanent magnet synchronous motor drive," in *2nd IEEE International Conference on Control, Instrumentation and Automation*, 2011, pp. 225–230.

[8] J. Bernat, J. Kolota, S. Stepien, and G. Szymanski, "Adaptive control of permanent magnet synchronous motor with constrained reference current exploiting backstepping methodology," in *the IEEE Conference on Control Applications*, 2014, pp. 1545–1550.

[9] V. Petrović, R. Ortega, and A. Stanković, "Interconnection and damping assignment approach to control of PM synchronous motors," *IEEE Trans. on Control Systems Technology*, vol. 9, no. 6, pp. 811–820, 2001.

[10] S. Bolognani, S. Bolognani, L. Peretti, and M. Zigliotto, "Design and implementation of Model Predictive Control for electrical motor drives," *IEEE Trans. on Industrial Electronics*, vol. 56, no. 6, pp. 1925–1936, 2009.

[11] T. Pham, I. Prodan, D. Genon-Catalot, and L. Lefèvre, "Efficient energy management for an elevator system under a constrained optimization framework," in *19th International Conference on System Theory, Control and Computing*, 2015, pp. 613 – 618.

[12] ——, "Port-Hamiltonian model for DC-microgrid lift systems," in *5th IFAC Workshop on Lagrangian and Hamiltonian Methods for Non Linear Control*, vol. 48, no. 13. Lyon, France: IFAC, July 2015, pp. 117–122.

[13] F. Stoican, I. Prodan, D. Popescu, and L. Ichim, "Constrained trajectory generation for UAV systems using a B-spline parametrization," in *25th Mediterranean Conference on Control and Automation*. Valletta, Malta: IEEE, July 2017.

[14] L. T. Biegler and V. M. Zavala, "Large-scale nonlinear programming using IPOPT: An integrating framework for enterprise-wide dynamic optimization," *Computers & Chemical Engineering*, vol. 33, no. 3, pp. 575–582, 2009.